

Measurements of neutral B decay branching fractions to $K_S^0\pi^+\pi^-$ final states

B. Aubert,¹ R. Barate,¹ D. Boutigny,¹ F. Couderc,¹ J.-M. Gaillard,¹ A. Hicheur,¹ Y. Karyotakis,¹ J. P. Lees,¹ V. Tisserand,¹ A. Zghiche,¹ A. Palano,² A. Pompili,² J. C. Chen,³ N. D. Qi,³ G. Rong,³ P. Wang,³ Y. S. Zhu,³ G. Eigen,⁴ I. Ofte,⁴ B. Stugu,⁴ G. S. Abrams,⁵ A. W. Borgland,⁵ A. B. Breon,⁵ D. N. Brown,⁵ J. Button-Shafer,⁵ R. N. Cahn,⁵ E. Charles,⁵ C. T. Day,⁵ M. S. Gill,⁵ A. V. Gritsan,⁵ Y. Groysman,⁵ R. G. Jacobsen,⁵ R. W. Kadel,⁵ J. Kadyk,⁵ L. T. Kerth,⁵ Yu. G. Kolomensky,⁵ G. Kukartsev,⁵ G. Lynch,⁵ L. M. Mir,⁵ P. J. Oddone,⁵ T. J. Orimoto,⁵ M. Pripstein,⁵ N. A. Roe,⁵ M. T. Ronan,⁵ V. G. Shelkov,⁵ W. A. Wenzel,⁵ M. Barrett,⁶ K. E. Ford,⁶ T. J. Harrison,⁶ A. J. Hart,⁶ C. M. Hawkes,⁶ S. E. Morgan,⁶ A. T. Watson,⁶ M. Fritsch,⁷ K. Goetzen,⁷ T. Held,⁷ H. Koch,⁷ B. Lewandowski,⁷ M. Pelizaeus,⁷ M. Steinke,⁷ J. T. Boyd,⁸ N. Chevalier,⁸ W. N. Cottingham,⁸ M. P. Kelly,⁸ T. E. Latham,⁸ F. F. Wilson,⁸ T. Cuhadar-Donszelmann,⁹ C. Hearty,⁹ N. S. Knecht,⁹ T. S. Mattison,⁹ J. A. McKenna,⁹ D. Thiessen,⁹ A. Khan,¹⁰ P. Kyberd,¹⁰ L. Teodorescu,¹⁰ A. E. Blinov,¹¹ V. E. Blinov,¹¹ V. P. Druzhinin,¹¹ V. B. Golubev,¹¹ V. N. Ivanchenko,¹¹ E. A. Kravchenko,¹¹ A. P. Onuchin,¹¹ S. I. Serednyakov,¹¹ Yu. I. Skovpen,¹¹ E. P. Solodov,¹¹ A. N. Yushkov,¹¹ D. Best,¹² M. Bruinsma,¹² M. Chao,¹² I. Eschrich,¹² D. Kirkby,¹² A. J. Lankford,¹² M. Mandelkern,¹² R. K. Mommsen,¹² W. Roethel,¹² D. P. Stoker,¹² C. Buchanan,¹³ B. L. Hartfiel,¹³ S. D. Foulkes,¹⁴ J. W. Gary,¹⁴ B. C. Shen,¹⁴ K. Wang,¹⁴ D. del Re,¹⁵ H. K. Hadavand,¹⁵ E. J. Hill,¹⁵ D. B. MacFarlane,¹⁵ H. P. Paar,¹⁵ Sh. Rahatlou,¹⁵ V. Sharma,¹⁵ J. W. Berryhill,¹⁶ C. Campagnari,¹⁶ B. Dahmes,¹⁶ O. Long,¹⁶ A. Lu,¹⁶ M. A. Mazur,¹⁶ J. D. Richman,¹⁶ W. Verkerke,¹⁶ T. W. Beck,¹⁷ A. M. Eisner,¹⁷ C. A. Heusch,¹⁷ J. Kroseberg,¹⁷ W. S. Lockman,¹⁷ G. Nesom,¹⁷ T. Schalk,¹⁷ B. A. Schumm,¹⁷ A. Seiden,¹⁷ P. Spradlin,¹⁷ D. C. Williams,¹⁷ M. G. Wilson,¹⁷ J. Albert,¹⁸ E. Chen,¹⁸ G. P. Dubois-Felsmann,¹⁸ A. Dvoretzki,¹⁸ D. G. Hitlin,¹⁸ I. Narsky,¹⁸ T. Piatenko,¹⁸ F. C. Porter,¹⁸ A. Ryd,¹⁸ A. Samuel,¹⁸ S. Yang,¹⁸ S. Jayatilake,¹⁹ G. Mancinelli,¹⁹ B. T. Meadows,¹⁹ M. D. Sokoloff,¹⁹ T. Abe,²⁰ F. Blanc,²⁰ P. Bloom,²⁰ S. Chen,²⁰ W. T. Ford,²⁰ U. Nauenberg,²⁰ A. Olivas,²⁰ P. Rankin,²⁰ J. G. Smith,²⁰ J. Zhang,²⁰ L. Zhang,²⁰ A. Chen,²¹ J. L. Harton,²¹ A. Soffer,²¹ W. H. Toki,²¹ R. J. Wilson,²¹ Q. L. Zeng,²¹ D. Altenburg,²² T. Brandt,²² J. Brose,²² M. Dickopp,²² E. Feltresi,²² A. Hauke,²² H. M. Lacker,²² R. Müller-Pfefferkorn,²² R. Nogowski,²² S. Otto,²² A. Petzold,²² J. Schubert,²² K. R. Schubert,²² R. Schwierz,²² B. Spaan,²² J. E. Sundermann,²² D. Bernard,²³ G. R. Bonneaud,²³ F. Brochard,²³ P. Grenier,²³ S. Schrenk,²³ Ch. Thiebaut,²³ G. Vasileiadis,²³ M. Verderi,²³ D. J. Bard,²⁴ P. J. Clark,²⁴ D. Lavin,²⁴ F. Muheim,²⁴ S. Playfer,²⁴ Y. Xie,²⁴ M. Andreotti,²⁵ V. Azzolini,²⁵ D. Bettoni,²⁵ C. Bozzi,²⁵ R. Calabrese,²⁵ G. Cibinetto,²⁵ E. Luppi,²⁵ M. Negrini,²⁵ L. Piemontese,²⁵ A. Sarti,²⁵ E. Treadwell,²⁶ F. Anulli,²⁷ R. Baldini-Ferrolì,²⁷ A. Calcaterra,²⁷ R. de Sangro,²⁷ G. Finocchiaro,²⁷ P. Patteri,²⁷ I. M. Peruzzi,²⁷ M. Piccolo,²⁷ A. Zallo,²⁷ A. Buzzo,²⁸ R. Capra,²⁸ R. Contri,²⁸ G. Crosetti,²⁸ M. Lo Vetere,²⁸ M. Macri,²⁸ M. R. Monge,²⁸ S. Passaggio,²⁸ C. Patrignani,²⁸ E. Robutti,²⁸ A. Santroni,²⁸ S. Tosi,²⁸ S. Bailey,²⁹ G. Brandenburg,²⁹ K. S. Chaisanguanthum,²⁹ M. Morii,²⁹ E. Won,²⁹ R. S. Dubitzky,³⁰ U. Langenegger,³⁰ W. Bhimji,³¹ D. A. Bowerman,³¹ P. D. Dauncey,³¹ U. Egede,³¹ J. R. Gaillard,³¹ G. W. Morton,³¹ J. A. Nash,³¹ M. B. Nikolich,³¹ G. P. Taylor,³¹ M. J. Charles,³² G. J. Grenier,³² U. Mallik,³² J. Cochran,³³ H. B. Crawley,³³ J. Lamsa,³³ W. T. Meyer,³³ S. Prell,³³ E. I. Rosenberg,³³ A. E. Rubin,³³ J. Yi,³³ M. Biasini,³⁴ R. Covarelli,³⁴ M. Pioppi,³⁴ M. Davier,³⁵ X. Giroux,³⁵ G. Grosdidier,³⁵ A. Höcker,³⁵ S. Laplace,³⁵ F. Le Diberder,³⁵ V. Lepeltier,³⁵ A. M. Lutz,³⁵ T. C. Petersen,³⁵ S. Piaszczyński,³⁵ M. H. Schune,³⁵ L. Tantot,³⁵ G. Wormser,³⁵ C. H. Cheng,³⁶ D. J. Lange,³⁶ M. C. Simani,³⁶ D. M. Wright,³⁶ A. J. Bevan,³⁷ C. A. Chavez,³⁷ J. P. Coleman,³⁷ I. J. Forster,³⁷ J. R. Fry,³⁷ E. Gabathuler,³⁷ R. Gamet,³⁷ D. E. Hutchcroft,³⁷ R. J. Parry,³⁷ D. J. Payne,³⁷ R. J. Sloane,³⁷ C. Touramanis,³⁷ J. J. Back,^{38,*} C. M. Cormack,³⁸ P. F. Harrison,^{38,*} F. Di Lodovico,³⁸ G. B. Mohanty,^{38,*} C. L. Brown,³⁹ G. Cowan,³⁹ R. L. Flack,³⁹ H. U. Flaecher,³⁹ M. G. Green,³⁹ P. S. Jackson,³⁹ T. R. McMahon,³⁹ S. Ricciardi,³⁹ F. Salvatore,³⁹ M. A. Winter,³⁹ D. Brown,⁴⁰ C. L. Davis,⁴⁰ J. Allison,⁴¹ N. R. Barlow,⁴¹ R. J. Barlow,⁴¹ P. A. Hart,⁴¹ M. C. Hodgkinson,⁴¹ G. D. Lafferty,⁴¹ A. J. Lyon,⁴¹ J. C. Williams,⁴¹ A. Farbin,⁴² W. D. Hulsbergen,⁴² A. Jawahery,⁴² D. Kovalskyi,⁴² C. K. Lae,⁴² V. Lillard,⁴² D. A. Roberts,⁴² G. Blaylock,⁴³ C. Dallapiccola,⁴³ K. T. Flood,⁴³ S. S. Hertzbach,⁴³ R. Kofler,⁴³ V. B. Koptchev,⁴³ T. B. Moore,⁴³ S. Saremi,⁴³ H. Staengle,⁴³ S. Willocq,⁴³ R. Cowan,⁴⁴ G. Sciolla,⁴⁴ S. J. Sekula,⁴⁴ F. Taylor,⁴⁴ R. K. Yamamoto,⁴⁴ D. J. J. Mangeol,⁴⁵ P. M. Patel,⁴⁵ S. H. Robertson,⁴⁵ A. Lazzaro,⁴⁶ V. Lombardo,⁴⁶ F. Palombo,⁴⁶ J. M. Bauer,⁴⁷ L. Cremaldi,⁴⁷ V. Eschenburg,⁴⁷ R. Godang,⁴⁷ R. Kroeger,⁴⁷ J. Reidy,⁴⁷ D. A. Sanders,⁴⁷ D. J. Summers,⁴⁷ H. W. Zhao,⁴⁷ S. Brunet,⁴⁸ D. Côté,⁴⁸ P. Taras,⁴⁸ H. Nicholson,⁴⁹ N. Cavallo,^{50,†} F. Fabozzi,^{50,†} C. Gatto,⁵⁰ L. Lista,⁵⁰ D. Monorchio,⁵⁰ P. Paolucci,⁵⁰ D. Piccolo,⁵⁰ C. Sciacca,⁵⁰ M. Baak,⁵¹ H. Bulten,⁵¹ G. Raven,⁵¹ H. L. Snoek,⁵¹ L. Wilden,⁵¹ C. P. Jessop,⁵² J. M. LoSecco,⁵² T. Allmendinger,⁵³ K. K. Gan,⁵³ K. Honscheid,⁵³ D. Hufnagel,⁵³ H. Kagan,⁵³ R. Kass,⁵³ T. Pulliam,⁵³ A. M. Rahimi,⁵³ R. Ter-Antonyan,⁵³ Q. K. Wong,⁵³ J. Brau,⁵⁴ R. Frey,⁵⁴ O. Igonkina,⁵⁴ C. T. Potter,⁵⁴ N. B. Sinev,⁵⁴ D. Strom,⁵⁴ E. Torrence,⁵⁴ F. Colecchia,⁵⁵

A. Dorigo,⁵⁵ F. Galeazzi,⁵⁵ M. Margoni,⁵⁵ M. Morandin,⁵⁵ M. Posocco,⁵⁵ M. Rotondo,⁵⁵ F. Simonetto,⁵⁵ R. Stroili,⁵⁵ G. Tiozzo,⁵⁵ C. Voci,⁵⁵ M. Benayoun,⁵⁶ H. Briand,⁵⁶ J. Chauveau,⁵⁶ P. David,⁵⁶ Ch. de la Vaissière,⁵⁶ L. Del Buono,⁵⁶ O. Hamon,⁵⁶ M. J. J. John,⁵⁶ Ph. Leruste,⁵⁶ J. Malcles,⁵⁶ J. Ocariz,⁵⁶ M. Pivk,⁵⁶ L. Roos,⁵⁶ S. T’Jampens,⁵⁶ G. Therin,⁵⁶ P. F. Manfredi,⁵⁷ V. Re,⁵⁷ P. K. Behera,⁵⁸ L. Gladney,⁵⁸ Q. H. Guo,⁵⁸ J. Panetta,⁵⁸ C. Angelini,⁵⁹ G. Batignani,⁵⁹ S. Bettarini,⁵⁹ M. Bondioli,⁵⁹ F. Bucci,⁵⁹ G. Calderini,⁵⁹ M. Carpinelli,⁵⁹ F. Forti,⁵⁹ M. A. Giorgi,⁵⁹ A. Lusiani,⁵⁹ G. Marchiori,⁵⁹ F. Martinez-Vidal,^{59,‡} M. Morganti,⁵⁹ N. Neri,⁵⁹ E. Paoloni,⁵⁹ M. Rama,⁵⁹ G. Rizzo,⁵⁹ F. Sandrelli,⁵⁹ J. Walsh,⁵⁹ M. Haire,⁶⁰ D. Judd,⁶⁰ K. Paick,⁶⁰ D. E. Wagoner,⁶⁰ N. Danielson,⁶¹ P. Elmer,⁶¹ Y. P. Lau,⁶¹ C. Lu,⁶¹ V. Miftakov,⁶¹ J. Olsen,⁶¹ A. J. S. Smith,⁶¹ A. V. Telnov,⁶¹ F. Bellini,⁶² G. Cavoto,^{61,62} R. Faccini,⁶² F. Ferrarotto,⁶² F. Ferroni,⁶² M. Gaspero,⁶² L. Li Gioi,⁶² M. A. Mazzoni,⁶² S. Morganti,⁶² M. Pierini,⁶² G. Piredda,⁶² F. Safai Tehrani,⁶² C. Voena,⁶² S. Christ,⁶³ G. Wagner,⁶³ R. Waldi,⁶³ T. Adye,⁶⁴ N. De Groot,⁶⁴ B. Franek,⁶⁴ N. I. Geddes,⁶⁴ G. P. Gopal,⁶⁴ E. O. Olaiya,⁶⁴ R. Aleksan,⁶⁵ S. Emery,⁶⁵ A. Gaidot,⁶⁵ S. F. Ganzhur,⁶⁵ P.-F. Giraud,⁶⁵ G. Hamel de Monchenault,⁶⁵ W. Kozanecki,⁶⁵ M. Legendre,⁶⁵ G. W. London,⁶⁵ B. Mayer,⁶⁵ G. Schott,⁶⁵ G. Vasseur,⁶⁵ Ch. Yèche,⁶⁵ M. Zito,⁶⁵ M. V. Purohit,⁶⁶ A. W. Weidemann,⁶⁶ J. R. Wilson,⁶⁶ F. X. Yumiceva,⁶⁶ D. Aston,⁶⁷ R. Bartoldus,⁶⁷ N. Berger,⁶⁷ A. M. Boyarski,⁶⁷ O. L. Buchmueller,⁶⁷ R. Claus,⁶⁷ M. R. Convery,⁶⁷ M. Cristinziani,⁶⁷ G. De Nardo,⁶⁷ D. Dong,⁶⁷ J. Dorfan,⁶⁷ D. Dujmic,⁶⁷ W. Dunwoodie,⁶⁷ E. E. Elsen,⁶⁷ S. Fan,⁶⁷ R. C. Field,⁶⁷ T. Glanzman,⁶⁷ S. J. Gowdy,⁶⁷ T. Hadig,⁶⁷ V. Halyo,⁶⁷ C. Hast,⁶⁷ T. Hryn’ova,⁶⁷ W. R. Innes,⁶⁷ M. H. Kelsey,⁶⁷ P. Kim,⁶⁷ M. L. Kocian,⁶⁷ D. W. G. S. Leith,⁶⁷ J. Libby,⁶⁷ S. Luitz,⁶⁷ V. Luth,⁶⁷ H. L. Lynch,⁶⁷ H. Marsiske,⁶⁷ R. Messner,⁶⁷ D. R. Muller,⁶⁷ C. P. O’Grady,⁶⁷ V. E. Ozcan,⁶⁷ A. Perazzo,⁶⁷ M. Perl,⁶⁷ S. Petrak,⁶⁷ B. N. Ratcliff,⁶⁷ A. Roodman,⁶⁷ A. A. Salnikov,⁶⁷ R. H. Schindler,⁶⁷ J. Schwiening,⁶⁷ G. Simi,⁶⁷ A. Snyder,⁶⁷ A. Soha,⁶⁷ J. Stelzer,⁶⁷ D. Su,⁶⁷ M. K. Sullivan,⁶⁷ J. Va’vra,⁶⁷ S. R. Wagner,⁶⁷ M. Weaver,⁶⁷ A. J. R. Weinstein,⁶⁷ W. J. Wisniewski,⁶⁷ M. Wittgen,⁶⁷ D. H. Wright,⁶⁷ A. K. Yarritu,⁶⁷ C. C. Young,⁶⁷ P. R. Burchat,⁶⁸ A. J. Edwards,⁶⁸ T. I. Meyer,⁶⁸ B. A. Petersen,⁶⁸ C. Roat,⁶⁸ S. Ahmed,⁶⁹ M. S. Alam,⁶⁹ J. A. Ernst,⁶⁹ M. A. Saeed,⁶⁹ M. Saleem,⁶⁹ F. R. Wappler,⁶⁹ W. Bugg,⁷⁰ M. Krishnamurthy,⁷⁰ S. M. Spanier,⁷⁰ R. Eckmann,⁷¹ H. Kim,⁷¹ J. L. Ritchie,⁷¹ A. Satpathy,⁷¹ R. F. Schwitters,⁷¹ J. M. Izen,⁷² I. Kitayama,⁷² X. C. Lou,⁷² S. Ye,⁷² F. Bianchi,⁷³ M. Bona,⁷³ F. Gallo,⁷³ D. Gamba,⁷³ L. Bosisio,⁷⁴ C. Cartaro,⁷⁴ F. Cossutti,⁷⁴ G. Della Ricca,⁷⁴ S. Dittongo,⁷⁴ S. Grancagnolo,⁷⁴ L. Lanceri,⁷⁴ P. Poropat,^{74,§} L. Vitale,⁷⁴ G. Vuagnin,⁷⁴ R. S. Panvini,⁷⁵ Sw. Banerjee,⁷⁶ C. M. Brown,⁷⁶ D. Fortin,⁷⁶ P. D. Jackson,⁷⁶ R. Kowalewski,⁷⁶ J. M. Roney,⁷⁶ R. J. Sobie,⁷⁶ H. R. Band,⁷⁷ B. Cheng,⁷⁷ S. Dasu,⁷⁷ M. Datta,⁷⁷ A. M. Eichenbaum,⁷⁷ M. Graham,⁷⁷ J. J. Hollar,⁷⁷ J. R. Johnson,⁷⁷ P. E. Kutter,⁷⁷ H. Li,⁷⁷ R. Liu,⁷⁷ A. Mihalyyi,⁷⁷ A. K. Mohapatra,⁷⁷ Y. Pan,⁷⁷ R. Prepost,⁷⁷ P. Tan,⁷⁷ J. H. von Wimmersperg-Toeller,⁷⁷ J. Wu,⁷⁷ S. L. Wu,⁷⁷ Z. Yu,⁷⁷ M. G. Greene,⁷⁸ and H. Neal⁷⁸

(BABAR Collaboration)

¹Laboratoire de Physique des Particules, F-74941 Annecy-le-Vieux, France

²Dipartimento di Fisica and INFN, Università di Bari, I-70126 Bari, Italy

³Institute of High Energy Physics, Beijing 100039, China

⁴Institute of Physics, University of Bergen, N-5007 Bergen, Norway

⁵Lawrence Berkeley National Laboratory and University of California, Berkeley, California 94720, USA

⁶University of Birmingham, Birmingham B15 2TT, United Kingdom

⁷Institut für Experimentalphysik I, Ruhr Universität Bochum, D-44780 Bochum, Germany

⁸University of Bristol, Bristol BS8 1TL, United Kingdom

⁹University of British Columbia, Vancouver, British Columbia, Canada V6T 1Z1

¹⁰Brunel University, Uxbridge, Middlesex UB8 3PH, United Kingdom

¹¹Budker Institute of Nuclear Physics, Novosibirsk 630090, Russia

¹²University of California at Irvine, Irvine, California 92697, USA

¹³University of California at Los Angeles, Los Angeles, California 90024, USA

¹⁴University of California at Riverside, Riverside, California 92521, USA

¹⁵University of California at San Diego, La Jolla, California 92093, USA

¹⁶University of California at Santa Barbara, Santa Barbara, California 93106, USA

¹⁷Institute for Particle Physics, University of California at Santa Cruz, Santa Cruz, California 95064, USA

¹⁸California Institute of Technology, Pasadena, California 91125, USA

¹⁹University of Cincinnati, Cincinnati, Ohio 45221, USA

²⁰University of Colorado, Boulder, Colorado 80309, USA

²¹Colorado State University, Fort Collins, Colorado 80523, USA

²²Institut für Kern- und Teilchenphysik, Technische Universität Dresden, D-01062 Dresden, Germany

²³Ecole Polytechnique, LLR, F-91128 Palaiseau, France

- ²⁴University of Edinburgh, Edinburgh EH9 3JZ, United Kingdom
- ²⁵Dipartimento di Fisica and INFN, Università di Ferrara, I-44100 Ferrara, Italy
- ²⁶Florida A&M University, Tallahassee, Florida 32307, USA
- ²⁷Laboratori Nazionali di Frascati dell'INFN, I-00044 Frascati, Italy
- ²⁸Dipartimento di Fisica and INFN, Università di Genova, I-16146 Genova, Italy
- ²⁹Harvard University, Cambridge, Massachusetts 02138, USA
- ³⁰Physikalisches Institut, Universität Heidelberg, Philosophenweg 12, D-69120 Heidelberg, Germany
- ³¹Imperial College London, London SW7 2AZ, United Kingdom
- ³²University of Iowa, Iowa City, Iowa 52242, USA
- ³³Iowa State University, Ames, Iowa 50011-3160, USA
- ³⁴Dipartimento di Fisica and INFN, Università di Perugia, I-06100 Perugia, Italy
- ³⁵Laboratoire de l'Accélérateur Linéaire, F-91898 Orsay, France
- ³⁶Lawrence Livermore National Laboratory, Livermore, California 94550, USA
- ³⁷University of Liverpool, Liverpool L69 7ZE, United Kingdom
- ³⁸Queen Mary, University of London, London E1 4NS, United Kingdom
- ³⁹University of London, Royal Holloway and Bedford New College, Egham, Surrey TW20 0EX, United Kingdom
- ⁴⁰University of Louisville, Louisville, Kentucky 40292, USA
- ⁴¹University of Manchester, Manchester M13 9PL, United Kingdom
- ⁴²University of Maryland, College Park, Maryland 20742, USA
- ⁴³University of Massachusetts, Amherst, Massachusetts 01003, USA
- ⁴⁴Laboratory for Nuclear Science, Massachusetts Institute of Technology, Cambridge, Massachusetts 02139, USA
- ⁴⁵McGill University, Montréal, Quebec, Canada H3A 2T8
- ⁴⁶Dipartimento di Fisica and INFN, Università di Milano, I-20133 Milano, Italy
- ⁴⁷University of Mississippi, University, Mississippi 38677, USA
- ⁴⁸Laboratoire René J. A. Lévesque, Université de Montréal, Montréal, Quebec, Canada H3C 3J7
- ⁴⁹Mount Holyoke College, South Hadley, Massachusetts 01075, USA
- ⁵⁰Dipartimento di Scienze Fisiche and INFN, Università di Napoli Federico II, I-80126, Napoli, Italy
- ⁵¹National Institute for Nuclear Physics and High Energy Physics, NIKHEF, NL-1009 DB Amsterdam, The Netherlands
- ⁵²University of Notre Dame, Notre Dame, Indiana 46556, USA
- ⁵³The Ohio State University, Columbus, Ohio 43210, USA
- ⁵⁴University of Oregon, Eugene, Oregon 97403, USA
- ⁵⁵Dipartimento di Fisica and INFN, Università di Padova, I-35131 Padova, Italy
- ⁵⁶Laboratoire de Physique Nucléaire et de Hautes Energies, Universités Paris VI et VII, F-75252 Paris, France
- ⁵⁷Dipartimento di Elettronica and INFN, Università di Pavia, I-27100 Pavia, Italy
- ⁵⁸University of Pennsylvania, Philadelphia, Pennsylvania 19104, USA
- ⁵⁹Dipartimento di Fisica, Scuola Normale Superiore and INFN, Università di Pisa, I-56127 Pisa, Italy
- ⁶⁰Prairie View A&M University, Prairie View, Texas 77446, USA
- ⁶¹Princeton University, Princeton, New Jersey 08544, USA
- ⁶²Dipartimento di Fisica and INFN, Università di Roma La Sapienza, I-00185 Roma, Italy
- ⁶³Universität Rostock, D-18051 Rostock, Germany
- ⁶⁴Rutherford Appleton Laboratory, Chilton, Didcot, Oxon, OX11 0QX, United Kingdom
- ⁶⁵DSM/Dapnia, CEA/Saclay, F-91191 Gif-sur-Yvette, France
- ⁶⁶University of South Carolina, Columbia, South Carolina 29208, USA
- ⁶⁷Stanford Linear Accelerator Center, Stanford, California 94309, USA
- ⁶⁸Stanford University, Stanford, California 94305-4060, USA
- ⁶⁹State University of New York, Albany, New York 12222, USA
- ⁷⁰University of Tennessee, Knoxville, Tennessee 37996, USA
- ⁷¹University of Texas at Austin, Austin, Texas 78712, USA
- ⁷²University of Texas at Dallas, Richardson, Texas 75083, USA
- ⁷³Dipartimento di Fisica Sperimentale and INFN, Università di Torino, I-10125 Torino, Italy
- ⁷⁴Dipartimento di Fisica and INFN, Università di Trieste, I-34127 Trieste, Italy
- ⁷⁵Vanderbilt University, Nashville, Tennessee 37235, USA
- ⁷⁶University of Victoria, Victoria, British Columbia, Canada V8W 3P6
- ⁷⁷University of Wisconsin, Madison, Wisconsin 53706, USA
- ⁷⁸Yale University, New Haven, Connecticut 06511, USA
- (Received 13 August 2004; published 11 November 2004)

*Now at Department of Physics, University of Warwick, Coventry, United Kingdom.

†Also with Università della Basilicata, Potenza, Italy.

‡Also with IFIC, Instituto de Física Corpuscular, CSIC-Universidad de Valencia, Valencia, Spain.

§Deceased.

Branching fraction measurements using B -meson decays to $K_S^0 \pi^+ \pi^-$ are presented. These measurements were obtained by analyzing a data sample of 88.9×10^6 $Y(4S) \rightarrow B\bar{B}$ decays collected with the $BABAR$ detector at the SLAC PEP-II asymmetric-energy B factory. Using a maximum likelihood fit, the following branching fraction results were obtained: $\mathcal{B}(B^0 \rightarrow K^0 \pi^+ \pi^-) = (43.7 \pm 3.8 \pm 3.4) \times 10^{-6}$, $\mathcal{B}(B^0 \rightarrow K^{*+} \pi^-) = (12.9 \pm 2.4 \pm 1.4) \times 10^{-6}$, and $\mathcal{B}(B^0 \rightarrow D^-(\rightarrow K_S^0 \pi^-) \pi^+) = (42.7 \pm 2.1 \pm 2.2) \times 10^{-6}$. The CP violating charge asymmetry $\mathcal{A}_{K^* \pi}$ for the decay $B^0 \rightarrow K^{*+} \pi^-$ was measured to be $\mathcal{A}_{K^* \pi} = 0.23 \pm 0.18_{-0.06}^{+0.09}$. For all these measurements the first error is statistical and the second is systematic.

DOI: 10.1103/PhysRevD.70.091103

PACS numbers: 13.25.Hw, 11.30.Er, 12.15.Hh

Three-body decays of the B meson tend to be dominated by intermediate quasi-two-body charmed particles with the charmless resonant and nonresonant contributions being small. Nevertheless, these charmless decays prove to be important in furthering our understanding of the weak interaction and complex quark couplings described by the Cabibbo-Kobayashi-Maskawa matrix elements [1].

The B -meson decay to $K_S^0 \pi^+ \pi^-$ can proceed via many interesting charmless resonances which we can probe for CP violation, such as $f_0 K_S^0$ [2], $\rho^0 K_S^0$, and $K^{*+} \pi^-$. A limit on the sum of their branching fractions can be obtained by measuring the inclusive charmless branching fraction of $B^0 \rightarrow K_S^0 \pi^+ \pi^-$. This measurement has been performed previously by the CLEO [3] and Belle [4] experiments. For the mode $B^0 \rightarrow K^{*+} \pi^-$ the branching fraction can be measured directly with the available $BABAR$ data sample.

Branching fraction and asymmetry measurements of charmless B decays can also be used to test the accuracy of QCD factorization models [5]. In particular there are factorization models that predict CP asymmetries in the decay $B^0 \rightarrow K^{*+} \pi^-$ [6]. The decay $B^0 \rightarrow K^{*+} \pi^-$ is self-tagged (the charge of the kaon reflects the flavor of the B meson), so the CP asymmetry can be defined as

$$\mathcal{A}_{K^* \pi} = \frac{\Gamma_{K^{*-} \pi^+} - \Gamma_{K^{*+} \pi^-}}{\Gamma_{K^{*-} \pi^+} + \Gamma_{K^{*+} \pi^-}}. \quad (1)$$

In this paper the branching fractions of $B^0 \rightarrow K^0 \pi^+ \pi^-$, $B^0 \rightarrow K^{*+} \pi^-$, and $B^0 \rightarrow D^-(\rightarrow K_S^0 \pi^-) \pi^+$ are presented, where charge conjugate decays are also implied. The procedure used selection criteria requiring events with a reconstructed $K_S^0 \pi^+ \pi^-$ final state. In the case of $\mathcal{B}(B^0 \rightarrow K^0 \pi^+ \pi^-)$, the total charmless contribution to the Dalitz plot was measured (with charmed and charmonium resonances removed), including contributions from resonant charmless substructures. For the decays $B^0 \rightarrow K^{*+} \pi^-$ and $B^0 \rightarrow D^-(\rightarrow K_S^0 \pi^-) \pi^+$, the analysis was restricted to the region of the $K_S^0 \pi^+ \pi^-$ Dalitz plot consistent with $K^{*+}(\rightarrow K_S^0 \pi^+)$ and $D^-(\rightarrow K_S^0 \pi^-)$ decays, respectively. Finally, the $\mathcal{A}_{K^* \pi}$ value for the decay $B^0 \rightarrow K^{*+} \pi^-$, which was first measured by CLEO [7] was extracted.

The data used in this analysis were collected at the PEP-II asymmetric-energy e^+e^- storage ring with the $BABAR$ detector [8]. The $BABAR$ detector consists of a

double-sided five-layer silicon tracker, a 40-layer drift chamber, a Cherenkov detector, an electromagnetic calorimeter, and a magnet with instrumented flux return. The data sample has an integrated luminosity of 81.9 fb^{-1} collected at the $Y(4S)$ resonance, which corresponds to $(88.9 \pm 1.0) \times 10^6$ $B\bar{B}$ pairs. It was assumed that the $Y(4S)$ decays equally to neutral and charged B -meson pairs. In addition, 9.6 fb^{-1} of data collected at 40 MeV below the $Y(4S)$ resonance were used for background studies.

Candidate B mesons were reconstructed from two tracks and a K_S^0 , where the K_S^0 was reconstructed from $\pi^+ \pi^-$ candidates. Each of the two tracks that were not generated by the K_S^0 were required to have at least 12 hits in the drift chamber, a transverse momentum greater than $100 \text{ MeV}/c$, and to be consistent with originating from the beam spot. These tracks were selected as pions using energy loss (dE/dx) measured in the tracking system, the number of photons measured by the Cherenkov detector, and their corresponding Cherenkov angle. Furthermore, the tracks were also required to fail the electron selection based on dE/dx information, the ratio of energy in the calorimeter to momentum in the drift chamber, and the shape of the signal in the calorimeter. The prerequisites imposed on K_S^0 candidates were for the reconstructed mass to be within $15 \text{ MeV}/c^2$ of the nominal K^0 mass [9], a decay vertex separated from the B^0 decay vertex by at least 5 standard deviations, and a cosine of the angle between the line joining the B and K_S^0 decay vertices and the K_S^0 momentum to be greater than 0.999.

To characterize signal events, two kinematic and one event-shape variable were used. The first kinematic variable ΔE is the difference between the center-of-mass (c.m.) energy of the B candidate and $\sqrt{s}/2$, where \sqrt{s} is the total c.m. energy. The second is the beam-energy-substituted mass $m_{ES} = \sqrt{(s/2 + \mathbf{p}_i \cdot \mathbf{p}_B)^2/E_i^2 - \mathbf{p}_B^2}$, where \mathbf{p}_B is the B momentum and (E_i, \mathbf{p}_i) is the four-momentum of the $Y(4S)$ in the laboratory frame. Using these two kinematic variables, candidates had to be in the range $|\Delta E| < 0.1 \text{ GeV}$ and $5.22 < m_{ES} < 5.29 \text{ GeV}/c^2$. The event-shape variable is a Fisher discriminant (\mathcal{F}) [10]. The \mathcal{F} variable was constructed from a linear combination of the cosine of the angle between the B -candidate momentum and the beam axis, the cosine

of the angle between the B -candidate thrust axis and the beam axis, and the energy flow of the rest of the event into each of nine contiguous, concentric, 10° cones around the thrust axis of the reconstructed B [11].

Continuum quark production ($e^+e^- \rightarrow q\bar{q}$ where $q = u, d, s, c$) was by far the dominant source of background. This was suppressed using another event-shape variable which was the cosine of the angle θ_T between the thrust axis of the selected B candidate and the thrust axis of the rest of the event. For continuum background, the distribution of $|\cos\theta_T|$ is strongly peaked towards unity whereas the distribution is flat for signal events. Therefore, the relative amount of continuum background was reduced by requiring that all candidates fulfill the criterion $|\cos\theta_T| < 0.9$.

Simulated Monte Carlo (MC) events were used to study background from other B -meson decays. The largest potential B background was seen to come from quasi-two-body decays including charmonium mesons such as $J/\psi K_S^0$, $\chi_{c0} K_S^0$, and $\psi(2S) K_S^0$ where the charmonium meson decays to $\mu^+\mu^-$ which are misidentified as pions or where they decay directly to $\pi^+\pi^-$. These background events were removed by vetoing reconstructed $\pi^+\pi^-$ masses consistent with $3.04 < m_{\pi^+\pi^-} < 3.17 \text{ GeV}/c^2$, $3.32 < m_{\pi^+\pi^-} < 3.53 \text{ GeV}/c^2$, and $3.60 < m_{\pi^+\pi^-} < 3.78 \text{ GeV}/c^2$, identifying the J/ψ , χ_{c0} , and $\psi(2S)$ mesons, respectively. Additionally, in order to measure the charmless branching fraction of the decay $B^0 \rightarrow K^0\pi^+\pi^-$, $B^0 \rightarrow D^-(\rightarrow K_S^0\pi^-)\pi^+$ events were removed by vetoing events with a reconstructed $K_S^0\pi$ invariant mass consistent with $1.83 < m_{K_S^0\pi} < 1.90 \text{ GeV}/c^2$. Monte Carlo simulation showed that $21 \pm 3 B^0 \rightarrow D^-(\rightarrow K_S^0\pi^-)\pi^+$ background events still remained. These events had a reconstructed D^- mass outside the veto as a result of using the wrong K_S^0 or π^+ which was incorrectly selected from the other B decay in the event. When selecting $B^0 \rightarrow K^{*+}\pi^-$ or $B^0 \rightarrow D^-(\rightarrow K_S^0\pi^-)\pi^+$ candidates, the additional cuts $0.79 < m_{K_S^0\pi} < 0.99 \text{ GeV}/c^2$ and $1.85 < m_{K_S^0\pi} < 1.89 \text{ GeV}/c^2$ were applied, respectively, to the reconstructed $m_{K_S^0\pi}$ invariant mass. After the above selection criteria were applied, a small proportion of events for all decays under study had more than one candidate which satisfied the selection criteria. For these events, one candidate alone was selected by choosing the candidate whose $\cos\theta_T$ value was closest to zero. In a signal MC study, this selects the true signal candidate more than 75% of the time.

After all cuts, the largest remaining B background to $B^0 \rightarrow K^0\pi^+\pi^-$ was the four-body decay $B^0 \rightarrow \eta' K_S^0$ with $\eta' \rightarrow \rho^0(770)\gamma$ and $\rho^0 \rightarrow \pi^+\pi^-$ which contributes 22 ± 6 events. For the $B^0 \rightarrow K^{*+}\pi^-$ and $B^0 \rightarrow D^-(\rightarrow K_S^0\pi^-)\pi^+$ channels, the background contribution was small and came from modes that can interfere by decaying to a $K_S^0\pi^+\pi^-$ final state such as $f_0 K_S^0$ and $\rho^0 K_S^0$. In

addition the $K^{*+}\pi^-$ and $D^+\pi^-$ modes are backgrounds to each other. Furthermore, there was the nonresonant $K_S^0\pi^+\pi^-$ background contribution to the resonant signal. Along with selection efficiencies obtained from MC, using available information on exclusive measurements [12] or by fitting to regions in the Dalitz plot, upper limits or branching fractions for these modes were obtained to estimate their background contributions.

In order to extract the signal event yield for the channel under study, an unbinned extended maximum likelihood fit was used. The likelihood function for N candidates is

$$\mathcal{L} = \exp\left(-\sum_{i=1}^M n_i\right) \prod_{j=1}^N \left(\sum_{l=1}^M n_l P_l(\vec{\alpha}, \vec{x}_j)\right), \quad (2)$$

where i, j , and l are integers, M is the number of hypotheses (signal, continuum background, and B background), $P_l(\vec{\alpha}, \vec{x}_j)$ is a probability density function (PDF) with the parameters $\vec{\alpha}$ depending on three variables (\vec{x}) m_{ES} , ΔE , and \mathcal{F} , and n_l is the number of events for each hypothesis determined by maximizing the likelihood function. The PDF is a product $P_l(\vec{\alpha}, \vec{x}_j) = P_l(\alpha_{m_{ES}}, m_{ES}) \cdot P_l(\alpha_{\Delta E}, \Delta E) \cdot P_l(\alpha_{\mathcal{F}}, \mathcal{F})$. Correlations between these variables were small for signal and continuum background hypotheses. However for B background, correlations were observed between m_{ES} and ΔE , which were taken into account by forming a two-dimensional PDF for these variables. The parameters of the signal and B -background PDFs were determined from MC. The continuum background parameters were allowed to vary in the fit, to help reduce systematic effects from this dominant event type. Upper sideband data defined to be in the region $0.1 < \Delta E < 0.3 \text{ GeV}$ and $5.22 < m_{ES} < 5.29 \text{ GeV}/c^2$ were used to model the continuum background PDFs. For the m_{ES} PDFs a Gaussian distribution was used for signal and a threshold function [13] was used for continuum. For the ΔE PDFs a sum of two Gaussian distributions with the same means was used for the signal and a first order polynomial was used for the continuum background. Finally, for the \mathcal{F} PDFs, a sum of two Gaussian distributions with distinct means and widths was used for signal and an asymmetric Gaussian which has different widths above and below the modal value was used for continuum background. In the case of B -background parametrizations, signal-like or continuum-like PDFs were used depending on the characteristics of the background. With more than 400 signal events and typically a one-to-one signal to background ratio in the total number of $B^0 \rightarrow D^-(\rightarrow K_S^0\pi^-)\pi^+$ candidates, it was possible also to vary the signal PDF parameters in the fit for this mode. This enabled uncertainties and corrections due to MC to be calculated and applied to the $B^0 \rightarrow K^0\pi^+\pi^-$ and $B^0 \rightarrow K^{*+}\pi^-$ analyses. Figure 1 shows the fitted projections of the maximum likelihood fit to $B^0 \rightarrow D^-(\rightarrow K_S^0\pi^-)\pi^+$ candidates in

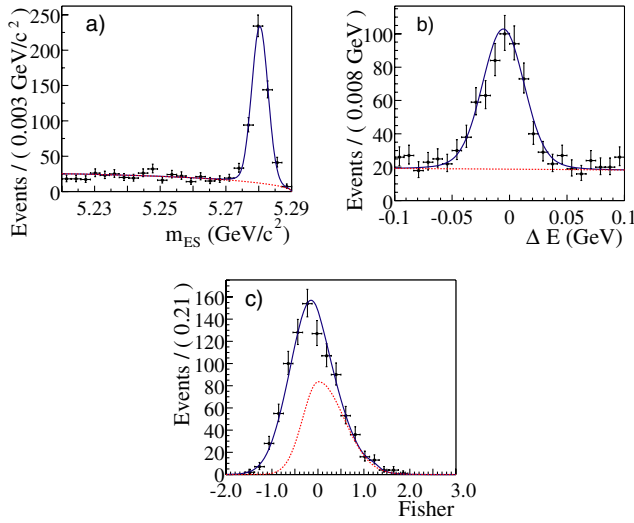


FIG. 1 (color online). Maximum likelihood fit projections of m_{ES} (a), ΔE (b), and \mathcal{F} (c) to the full set of $B^0 \rightarrow D^- (\rightarrow K_S^0 \pi^-) \pi^+$ candidates. The dashed lines are the fitted background PDFs while the solid continuous lines are the sums of the signal and background PDFs. The solid dots are data used in the fit.

m_{ES} , ΔE , and \mathcal{F} containing 472 ± 24 signal and 455 ± 23 background candidates.

To extract the branching fractions for the decay modes $B^0 \rightarrow K^{*+} \pi^-$ and $B^0 \rightarrow D^- (\rightarrow K_S^0 \pi^-) \pi^+$ the following equation was used:

$$\mathcal{B} = \frac{n_{\text{sig}}}{N_{BB} \times \epsilon}, \quad (3)$$

where n_{sig} is the number of signal events fitted, ϵ is the signal efficiency obtained from MC, and N_{BB} is the total number of $B\bar{B}$ events. For the charmless inclusive $B^0 \rightarrow K^0 \pi^+ \pi^-$ branching fraction, the efficiency varies over the Dalitz plane and the distribution of events across it is *a priori* unknown, consequently the total efficiency is unknown. Therefore, to calculate the branching fraction, a weight was assigned to each event such that for the j th event $\mathcal{W}_j = \sum_i V_{\text{sig},i} P_i(\vec{\alpha}, \vec{x}_j) / \sum_k n_k P_k(\vec{\alpha}, \vec{x}_j)$ where $V_{\text{sig},i}$ is the signal row of the covariance matrix obtained from the fit [14]. This procedure is effectively a background subtraction where these weights have the property $\sum_j \mathcal{W}_j = n_{\text{sig}}$. The branching fraction is then calculated as $\mathcal{B} = \sum_j \mathcal{W}_j / (\epsilon_j \times N_{BB})$ where ϵ_j is the efficiency which varies across the Dalitz plot and is simulated in small bins using high statistics MC.

Figure 2 shows the fitted projections for both $B^0 \rightarrow K^0 \pi^+ \pi^-$ and $B^0 \rightarrow K^{*+} \pi^-$ candidates, while the fitted signal yield and measured branching fraction are shown in Table I for all the modes under study. Figure 3 shows the signal mass projections of $m_{K_S^0 \pi}$ using $B^0 \rightarrow K^0 \pi^+ \pi^-$ candidates. The $m_{K_S^0 \pi}$ distribution clearly shows a peak at

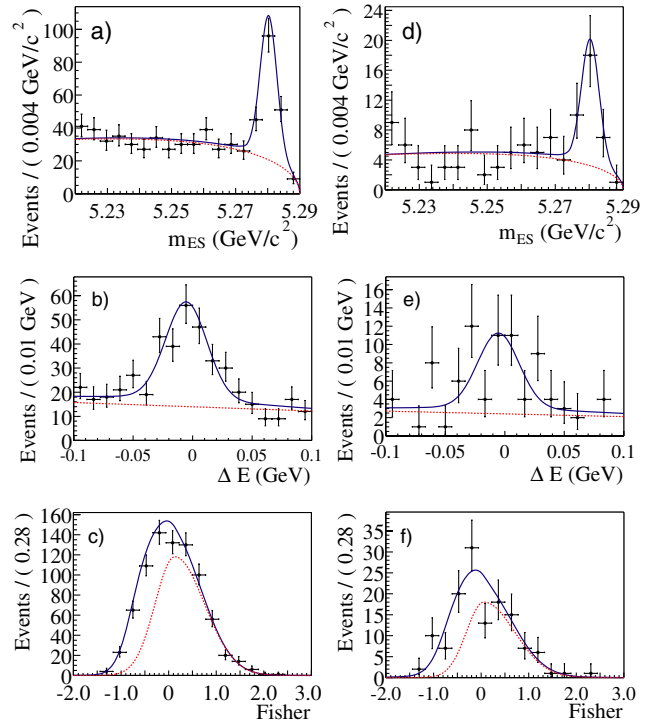


FIG. 2 (color online). Maximum likelihood fit projections of m_{ES} , ΔE , and \mathcal{F} for signal enhanced samples of charmless $B^0 \rightarrow K^0 \pi^+ \pi^-$ and $B^0 \rightarrow K^{*+} \pi^-$ candidates. The dashed lines are the fitted background PDFs while the solid continuous lines are the sums of the signal and background PDFs. The solid dots are data. (a)–(c) have the $B^0 \rightarrow K^0 \pi^+ \pi^-$ projections and the (d)–(f) have the $B^0 \rightarrow K^{*+} \pi^-$ projections, the top, middle, and bottom rows being the m_{ES} , ΔE , and \mathcal{F} distributions, respectively.

$0.9 \text{ GeV}/c^2$ which corresponds to the K^{*+} (892) and there is a broad structure above $1 \text{ GeV}/c^2$ which is the region where higher kaon resonances can occur.

Contributions to the branching fraction systematic error are shown in Table II. Errors due to pion tracking, particle identification, and K_S^0 reconstruction efficiency were assigned by comparing control channels in MC and data. To calculate errors due to the fit procedure, a large number of MC samples containing the amounts of signal, continuum, and B -background events measured or fixed in data were used. The differences between the generated and fitted values using these samples were used to ascertain the sizes of any biases. Small biases of the order of a few percent were observed that were a consequence of small correlations between fit variables and were therefore assigned as systematic errors. The uncertainty of the B -background contribution to the fit was estimated by varying the measured branching fractions within their errors. Each background was varied individually and the effect on the fitted signal yield was added as a contribution to the uncertainty. The $K_S^0 \pi^+ \pi^-$ nonresonant rate

TABLE I. Signal yields, efficiencies, and branching fractions for $B^0 \rightarrow K^0 \pi^+ \pi^-$, $B^0 \rightarrow K^{*+} \pi^-$, and $B^0 \rightarrow D^- (\rightarrow K_S^0 \pi^-) \pi^+$ where the first error is statistical and in the case of the measured branching fractions the second error is systematic. The $B^0 \rightarrow K^{*+} \pi^-$ branching fraction takes into account that $\mathcal{B}(K^{*+} \rightarrow K^0 \pi^+) = 2/3$, assuming isospin symmetry.

Mode	Signal events yield	Efficiency (%)	Measured branching fraction ($\times 10^{-6}$)	World average branching fraction ($\times 10^{-6}$)
$B^0 \rightarrow K^0 \pi^+ \pi^-$	310 ± 27	8.0	$43.7 \pm 3.8 \pm 3.4$	47 ± 7
$B^0 \rightarrow K^{*+} \pi^-$	59 ± 11	5.1	$12.9 \pm 2.4 \pm 1.4$	16^{+6}_-5
$B^0 \rightarrow D^- (\rightarrow K_S^0 \pi^-) \pi^+$	472 ± 24	12.4	$42.7 \pm 2.1 \pm 2.2$	41.7 ± 6.2

was assumed to be flat across the Dalitz plot and an upper limit for it was calculated by fitting to the region $2.0 < m_{\pi\pi} < 3.0 \text{ GeV}/c^2$. This corresponded to a 90% confidence level upper limit of 5.58×10^{-6} which was then used to calculate the background to the resonant modes and added as a systematic. For $B^0 \rightarrow K^{*+} \pi^-$ there was also the B -background contributions from higher kaon resonances which was added as a systematic and modeled using a Breit-Wigner. This was seen to be a conservative systematic, as the higher kaon resonance model overestimated events at low invariant mass. The uncertainty due to simulated PDFs was obtained from the channel $B^0 \rightarrow D^- (\rightarrow K_S^0 \pi^-) \pi^+$ and by varying the PDFs according to the precision of the parameters obtained from MC. In order to take correlations between parameters into account, the full correlation matrix was used when varying parameters. All PDF parameters that were originally fixed in the fit were then varied in turn and each difference from the nominal fit was combined and taken as a systematic contribution. The error in the efficiency was due to limited MC statistics, where over $\times 10^6$ MC events

were generated for the decay $B^0 \rightarrow K^0 \pi^+ \pi^-$ and over 150 000 MC events were generated for the decays $B^0 \rightarrow K^{*+} \pi^-$ and $B^0 \rightarrow D^- (\rightarrow K_S^0 \pi^-) \pi^+$. The same uncertainty due to the error in the number of $B\bar{B}$ events was added to all channels.

Interference was also considered for the decay $B^0 \rightarrow K^{*+} \pi^-$ where effects between the $K^{*+}(892)$ and S wave final states [nonresonant and $K_0^{*+}(1430)$] cancel and the $K^{*+}(892)$ and D wave final states [$K_2^{*+}(1430)$] cancel [15]. This is not the case for P wave amplitudes such as $K_1^{*+}(1410)$, yet this effect was considered negligible due to the small branching fraction of $K_1^{*+}(1410) \rightarrow K_S^0 \pi^+$ ($6.6\% \pm 1.3\%$ [9]).

The CP violating charge asymmetry for the decay $B^0 \rightarrow K^{*+} \pi^-$ was measured to be $\mathcal{A}_{K^* \pi} = 0.23 \pm 0.18^{+0.09}_{-0.06}$, where the first error is statistical and the second errors are systematic. The background asymmetry $\mathcal{A}_{K^* \pi}^{Bkg}$ was measured to be 0.01 ± 0.01 and as a further study the asymmetry $\mathcal{A}_{D\pi}$ for $B^0 \rightarrow D^- (\rightarrow K_S^0 \pi^-) \pi^+$ was measured to be 0.00 ± 0.05 and the background asymmetry $\mathcal{A}_{D\pi}^{Bkg}$ was 0.06 ± 0.04 , where the errors are statistical only.

The systematic error on $\mathcal{A}_{K^* \pi}$ was calculated by considering contributions due to track finding, particle identification, fit biases, and B -background asymmetry uncertainties. Biases due to track finding and particle identification were found to be negligible. The fit bias

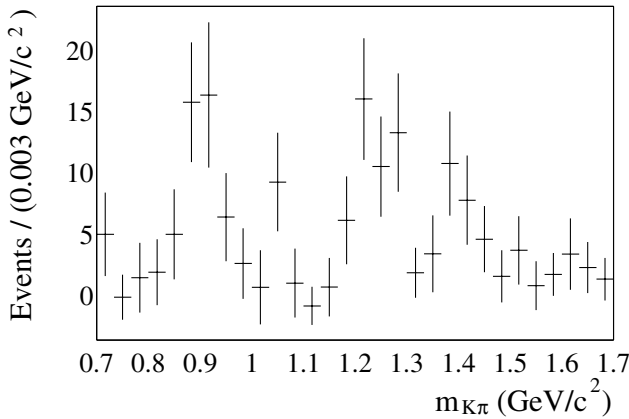


FIG. 3. The $m_{K\pi}$ distribution of $B^0 \rightarrow K^0 \pi^+ \pi^-$ candidates, weighted by \mathcal{W} such that background events are subtracted. The one-dimensional distribution is obtained by considering events on a Dalitz plane with axes $m_{K_S^0 \pi^+}^2$ and $m_{K_S^0 \pi^-}^2$. The two axes are merged into one ($m_{K\pi}^2$) by folding the Dalitz plane along the line corresponding to $m_{K_S^0 \pi^+}^2 = m_{K_S^0 \pi^-}^2$ in order to obtain the above $m_{K\pi}$ mass distribution.

TABLE II. Summary of systematic uncertainty contributions to the branching fraction measurements $B^0 \rightarrow K^0 \pi^+ \pi^-$, $B^0 \rightarrow K^{*+} \pi^-$, and $B^0 \rightarrow D^- (\rightarrow K_S^0 \pi^-) \pi^+$. The errors are shown as a percentage of the measured branching fraction.

Error source	$B^0 \rightarrow K^0 \pi^+ \pi^-$ Error (%)	$B^0 \rightarrow K^{*+} \pi^-$ Error (%)	$B^0 \rightarrow D^- \pi^+$ Error (%)
Tracking	1.7	1.7	1.7
Particle identification	1.9	1.2	3.0
K_S^0 efficiency	4.2	3.5	3.0
Fit bias	4.1	3.3	1.8
B background	3.6	9.0	0.3
PDF parameters	1.5	0.5	0.4
Efficiency	1.7	0.6	0.6
No. of $B\bar{B}$	1.1	1.1	1.1
Total	7.8	10.5	5.1

B. AUBERT *et al.*

contribution to the systematic error was calculated using a large number of MC samples. The contribution from B background was calculated by varying the number of expected events within errors and by assuming a conservative CP violating asymmetry of ± 0.5 as there are no available measurements for these decays. The resulting systematic uncertainty on the asymmetry was measured to be $^{+0.09}_{-0.06}$.

In summary, the branching fractions for $B^0 \rightarrow K^0 \pi^+ \pi^-$, $B^0 \rightarrow K^{*+} \pi^-$, and $B^0 \rightarrow D^- (\rightarrow K_S^0 \pi^-) \pi^+$ decaying to a $K_S^0 \pi^+ \pi^-$ state have been measured and agree with previous measurements [3,4,9]. The direct CP violating parameter $\mathcal{A}_{K^* \pi}$ was measured for the decay $B^0 \rightarrow K^{*+} \pi^-$ and is in agreement with the CLEO measurement [7], with no evidence of CP violation with the statistics used. Using larger data sets, one can extract amplitudes and relative phases of the resonant contribu-

tions to the Dalitz plot, with the possibility to observe new B -meson decays.

We are grateful for the excellent luminosity and machine conditions provided by our PEP-II colleagues and for the substantial dedicated effort from the computing organizations that support *BABAR*. The collaborating institutions wish to thank SLAC for its support and kind hospitality. This work is supported by DOE and NSF (USA), NSERC (Canada), IHEP (China), CEA and CNRS-IN2P3 (France), BMBF and DFG (Germany), INFN (Italy), FOM (The Netherlands), NFR (Norway), MIST (Russia), and PPARC (United Kingdom). Individuals have received support from CONACyT (Mexico), the A. P. Sloan Foundation, the Research Corporation, and the Alexander von Humboldt Foundation.

-
- [1] N. Cabibbo, Phys. Rev. Lett. **10**, 531 (1963); M. Kobayashi and T. Maskawa, Prog. Theor. Phys. **49**, 652 (1973).
- [2] *BABAR* Collaboration, B. Aubert *et al.*, hep-ex/0406040.
- [3] CLEO Collaboration, E. Eckhart *et al.*, Phys. Rev. Lett. **89**, 251801 (2002).
- [4] Belle Collaboration, A. Garmash *et al.*, Phys. Rev. D **69**, 012001 (2004).
- [5] M. Beneke and M. Neubert, Nucl. Phys. **B675**, 333 (2003).
- [6] Z. Xiao, W. Li, L. B. Guo, and G. Lu, Eur. Phys. J. C **18**, 681 (2001).
- [7] CLEO Collaboration, B. I. Eisenstein *et al.*, Phys. Rev. D **68**, 017101 (2003).
- [8] *BABAR* Collaboration, B. Aubert *et al.*, Nucl. Instrum. Methods Phys. Res., Sect. A **479**, 1 (2002).
- [9] Particle Data Group, S. Eidelman *et al.*, Phys. Lett. B **592**, 1 (2004).
- [10] R. A. Fisher, Ann. Eugenics **7**, 179 (1936); G. Cowan, *Statistical Data Analysis* (Oxford University Press, New York, 1998), p. 51.
- [11] CLEO Collaboration, D. M. Asner *et al.*, Phys. Rev. D **53**, 1039 (1996).
- [12] The Heavy Flavor Averaging Group (HFAG), <http://www.slac.stanford.edu/xorg/hfag/>
- [13] ARGUS Collaboration, H. Albrecht *et al.*, Z. Phys. C **48**, 543 (1990).
- [14] M. Pivk and F. R. Le Diberder, physics/0402083.
- [15] As is the case here for $K^{*+}(892)$, the cancellation requires the efficiency to be uniform along the mass distribution in the Dalitz plot.